Winglet Effects on the Flutter of a Twin-Engine Transport-Type Wing

Kumar G. Bhatia* and K. S. Nagaraja†
Boeing Commercial Airplane Company, Seattle, Washington
and
Charles L. Ruhlin‡
NASA Langley Research Center, Hampton, Virginia

Flutter characteristics of a cantilevered high aspect ratio wing with winglet were investigated. The configuration represented a current-technology, twin-engine airplane. Low- and high-speed models were used to evaluate compressibility effects through transonic Mach numbers and a wide range of mass-density ratios. Four flutter mechanisms were obtained in test and analysis from various combinations of configuration parameters. The coupling between wing-tip vertical and chordwise motions was shown to have a significant effect under some conditions. It is concluded that, for the flutter model configurations studied, the winglet-related flutter was amenable to the conventional flutter analysis techniques.

Introduction

THE interest in using wing-tip-mounted winglets to reduce drag for transport airplanes was stimulated by the work reported in Ref. 1. One of the first applications of winglets was for the KC-135 airplane based on a potential drag reduction of about 6% as estimated in Ref. 2. The KC-135 Winglet Flight Research and Demonstration Program was formulated to design, fabricate, and flight test a set of winglets to prove the drag reduction and other characteristics of the winglet concept. This program included a low-speed wind tunnel flutter model test and a flight flutter test program.[3] The critical mode during flight flutter test was a 3.0-Hz low-damped mode occurring with a light fuel loading at an altitude of 21,500 ft with a 0-deg cant angle and −4 deg incidence winglets. Flight testing for this configuration was terminated at 370 keas, rather than the test goal of 395 keas, due to low damping ($g=0.015$). The low damping obtained for this mode was not predicted by flutter analysis. The lack of correlation was judged to be due to limitations of current linearized aerodynamic theory and inability to represent transonic effects. Winglets have also been considered for the B-747 airplane as a part of the NASA Energy Efficient Transport Program.[4] Two flutter modes were obtained in the low-speed model test for the configuration with winglets. These flutter mechanisms were not present for the baseline configuration without winglets and were shown to result from winglet aerodynamics rather than mass effects. Flutter speeds for the configuration with winglets were significantly lower than the baseline configuration. It was suggested that the flutter mechanisms could be predicted by incorporating static-lift effects as with T-tail-type flutter analysis.

A transonic flutter model study of a supercritical wing with winglets for an executive jet-transport airplane[5] reported a good analysis/test correlation. The winglet addition decreased flutter speed by 7%, of which a 5% decrease was due to the wing-tip mass effect. Thus, there was no significant reduction in flutter speed due to winglet aerodynamics. Results of another application of winglets for the DC-10 airplane under the NASA Energy Efficient Transport Program were published recently.[6,7] A low-speed flutter model test showed that the winglets had generally detrimental effects on the flutter characteristics with small-to-moderate degradation in the basic wing flutter mode and a large degradation in a higher frequency wing flutter mode. During the flight test of the DC-10 airplane with winglets, mass balance of 500 lb was installed in each wing tip to ensure adequate flutter margins for flight testing.

It appears from the available data that winglets generally caused degradation in flutter speed. The actual reduction in flutter speed varied with the configuration. The KC-135 flight-test experience of encountering an unexpected low-damped mode highlighted the technical risk involved in flutter assessment of an airplane configuration with winglets. The only transonic wind tunnel flutter test data available on a scaled airplane wing was for an executive jet-transport wing[5] which showed a small reduction in flutter speed due to the addition of a winglet. These considerations led to a joint Boeing/NASA program to develop a flutter methodology for winglet-configured wings. A typical, current-technology, twin-engine-transport wing was selected as the basis for the study. A test program was outlined as follows:

1) Pressure Model Test for Aerodynamic Data Base
2) Low-Speed Test
   a) Model Ground Vibration Test (GVT)
   b) Flutter Test and Parametric Studies
   c) Analysis/Test Correlation
3) Test in NASA Langley 16 ft Transonic Dynamics Tunnel (TDT)
   a) Retest of Low-Speed Flutter Model for Mass-Density Ratio Effects
   b) Selection of High-Speed Model Configurations
   c) High-Speed Model GVT
   d) High-Speed Model Flutter Test
   e) Analysis/Test Correlation

Presented as Paper 84-0905 at the AIAA/ASME/ASCE/AHS 25th Structures, Structural Dynamics and Materials Conference, Palm Springs, Calif., May 14-16, 1984; received Aug. 18, 1984; revision received March 11, 1985.

*Senior Specialist Engineer, Flutter, New Product Development. Associate Fellow AIAA.
†Specialist Engineer, Flutter, New Product Development. Member AIAA.
‡Aerospace Technologist, Configuration Aeroelasticity Branch. Member AIAA.

Cantilevered wing models were used in all three tests. It was judged that once the wing/winglet interaction was represented adequately, the effect of body and empennage on flutter could be accounted for.

The details of this program are reported in Refs. 8 and 9. A summary of the program is discussed subsequently.

Test Configurations and Parameters

The choice of flutter test configurations and parameters was dictated by the task definition, viz., to develop flutter methodology. Therefore, the test was planned to obtain different kinds of flutter modes so that the winglet mass and aerodynamic effects could be identified separately for each of the flutter modes. The low-speed flutter test was designed with a larger number and a wider range of parameters taking advantage of the relative ease of atmospheric low-speed flutter testing compared to high-speed testing. The high-speed flutter test was designed after establishing analysis/test correlation for the low-speed flutter test. Based on the knowledge derived from the low-speed flutter test, a reduced number of configurations and parameters were selected for testing in the high-speed tunnel. The low-speed flutter test was conducted at the General Dynamics, Convair Division, San Diego, wind tunnel facility. The transonic test was conducted in the NASA Langley 16 ft TDT. A schematic diagram of the wing and wing tips tested is shown in Fig. 1.

Low-Speed Test

The low-speed model wing was of conventional single-spar construction with the wing sections perpendicular to the spar. The configurations for the low-speed flutter model test were:

1) a) Clean wing (without nacelle), b) Wing with winglet (without nacelle), and c) Wing with winglet mass simulator (without nacelle).

2) a) Wing with nacelle, b) Wing with nacelle and winglet, and c) Wing with nacelle and winglet mass simulator.

3) a) Wing with nacelle boom, b) Wing with nacelle boom and winglet, and c) Wing with nacelle boom and winglet mass simulator.

The winglet mass simulator was designed to represent winglet weight, center of gravity, and inertia properties to help separate winglet inertia and aerodynamic effects. The results from configurations with nacelle boom were not used due to good correlation obtained for the configurations with nacelle. The parameters varied were: 1) angle of attack; 2) model yaw angle; 3) wing fuel (0, 50, 75, and 100%); 4) nacelle strut side-bending frequency; 5) nacelle strut vertical-bending frequency; 6) winglet/simulator cant angle (0, 10, and 20 deg relative to the vertical); and 7) winglet/simulator stiffness. The variation of angle of attack and yaw angle was included to evaluate the static-lift effects.

NASA Langley TDT Test

The main objective of flutter testing in the NASA Langley TDT was to determine the effects of Mach number on flutter characteristics. However, the flutter points obtained in a variable-density, transonic tunnel depend upon the mass-density ratio as well as the Mach effects. Therefore, the low-speed model was retested in TDT to determine altitude or mass-density ratio effects at low speeds. Only two configurations—empty wing with nominal nacelle and with and without winglet—were tested. The analysis had shown a switch in flutter mode from nacelle vertical bending to second wing bending due to a decrease in the mass-density ratio. To obtain the mode change in the tunnel, mass-density ratio was varied by testing the configuration with the winglet in both air and freon. The strategy was to show that the mass-density ratio effects for a winglet-configured wing could be predicted at low Mach numbers. The flutter correlation at higher Mach numbers then could be evaluated on the basis of compressibility and transonic effects. The high-speed model was tested in freon for a Mach range of approximately 0.6-0.91 and dynamic pressures up to 200 psf.

The high-speed model was constructed primarily of fiberglass sandwich components with ribs, spars, stringers, and skin representing a modern transport wing. The wing fuel was simulated by water. The model was instrumented with 20 accelerometers, 23 pressure transducers in two chordwise arrays, and strain gages to monitor wing and winglet loads. The following configurations were selected for testing: 1) wing with nacelle and nominal tip, 2) wing with nacelle and ballasted tip, and 3) wing with nacelle and winglet.

The ballasted-tip configuration was selected to determine the effect of winglet weight separately from winglet aerodynamics. A winglet mass simulator similar to that used on the low-speed model would have introduced unknown aerodynamic effects at high speeds. Therefore, the ballast weight was incorporated inside the wing contour resulting in a wing tip aerodynamically identical to the nominal tip. The test parameters selected were 1) wing fuel (empty and full), 2) nacelle strut vertical-bending frequency, 3) winglet cant angle (0 and 20 deg relative to the vertical), and 4) angle of attack. Two nacelle strut vertical-bending springs were used. The nominal strut vertical-bending spring (nominal nacelle) and the softer strut vertical-bending spring (soft nacelle) gave rise to different flutter characteristics due to differences in coupling of nacelle motion with inboard wing torsion. A series of high-angle-of-attack runs within the model load limits was run to verify that there were no single-degree-of-freedom instabilities at transonic speeds.

Low-Speed Flutter Results

Model GVT

The model ground vibration test (GVT) was performed to establish analysis/test correlation for the model frequencies

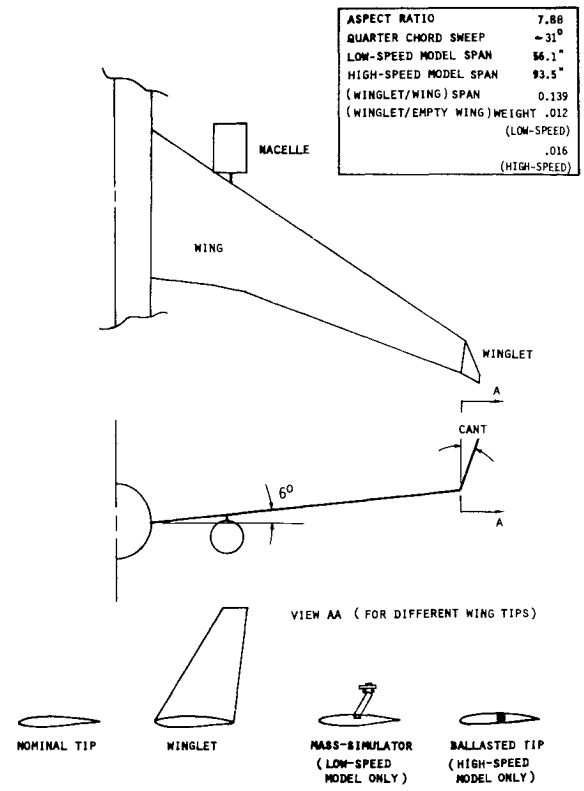

Fig. 1 Model wing and wing tips.

and mode shapes. The results of modal correlation for the 75% fuel case are shown in Figs. 2a and 2b for configurations with and without winglet, respectively. The agreement between the analysis and test was judged to be satisfactory.

Modal damping for the model was determined from the GVT. Structural damping (g) for the modes expected to flutter was about 0.005, except for the nacelle vertical-bending mode. The nacelle vertical-bending mode had structural damping of about 0.015.

Flutter Test Results

A total of four flutter modes were observed during the flutter test. The flutter modes observed were categorized as follows:

1) The basic nacelle vertical-bending (NVB) mode was characterized by relatively large nacelle and wing-tip vertical motions. The flutter frequency of this mode was in the 8.3-8.7-Hz range except with 100% fuel where this mode, when it occurred, had a frequency of 6.6-6.7 Hz.

2) The wing-tip (WT) mode was characterized by high frequency and sudden flutter onset. It was a classic type of flutter mode where the wing bending and first torsion modes coalesce into a mode with rapidly reducing damping level and frequency. When encountered for the clean wing configuration, the flutter frequency ranged from 12 to 22 Hz. For configurations with nacelle or nacelle and winglet, the frequency was approximately 14 Hz. The oscillograph traces for the 14-Hz mode showed wing-tip chordwise motion almost in phase with wing-tip vertical motion.

3) The second wing-bending (WB2) mode occurred only with winglet or simulator for certain fuel and nacelle vertical-bending combinations. It was characterized by flutter frequency in the 10-12-Hz range. The wing-tip chordwise motion was seen to be distinctly harmonic and of similar amplitude as the wing-tip vertical motion for winglet configurations. For simulator configurations, the wing-tip chordwise motion was not evident.

4) The combination wing chordwise and tip (WCT) mode was characterized by the prominence of a 10.0-Hz wing chordwise mode along with a higher wing frequency mode of about 14-15 Hz (in the autospectra from the wing-tip vertical accelerometer). For several runs, it appeared that the chordwise motion first increased with speed and then decreased before the tunnel was shut down due to excessive wing-tip vertical response. This flutter mode appeared only for the 100% fuel condition.

Figure 3 summarizes the test results for the three wing-tip configurations. Flutter characteristics for the three partial fuel cases (0, 50, and 75% fuel) were similar to each other and the flutter speeds were within about 3 ktas of each other. The flutter characteristics of partial fuel cases were different from the full fuel case. For partial fuel with nominal nacelle, the flutter mode remained as the basic NVB mode. The flutter speed with the simulator tip increased by about 6% over the nominal tip. However, with the winglet tip, the flutter speed decreased by about 13% relative to the flutter speed with the simulator tip. With the soft nacelle configuration, the flutter mode changed from the WT mode for the nominal tip to the WB2 mode for the simulator and winglet tips. The flutter speed with the simulator tip decreased by about 5% relative to the nominal tip. The winglet tip reduced the flutter speed by about 19% relative to the simulator tip.

For configurations with full fuel and either nominal or soft nacelle, flutter occurred in the basic NVB mode at about the same speed for both the nominal and simulator wing tips. However, the flutter mode changed to the WT mode with the winglet tip, and the speed was lower by about 7% relative to the simulator tip.

In all cases the winglet's effect was to significantly reduce the flutter speed. The winglet mass effect was to either increase or slightly decrease the flutter speed. Hence, the major contributor to the reduction in flutter speed was winglet aerodynamics.

The effect of cant angle for the simulator configurations was found to be insignificant. However, for the winglet configurations, increasing the cant angle reduced the flutter speed. This suggests that the primary effect is due to the

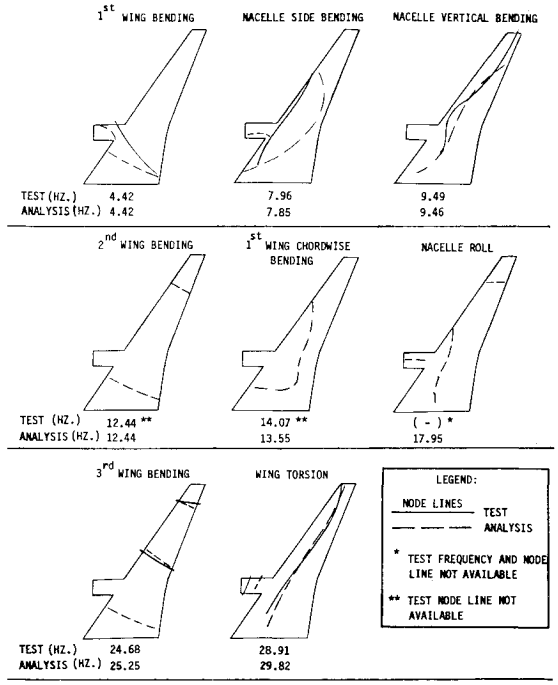

Fig. 2a Still air vibration correlation for low-speed model wing (75% fuel)/nacelle (nominal)/nominal tip.

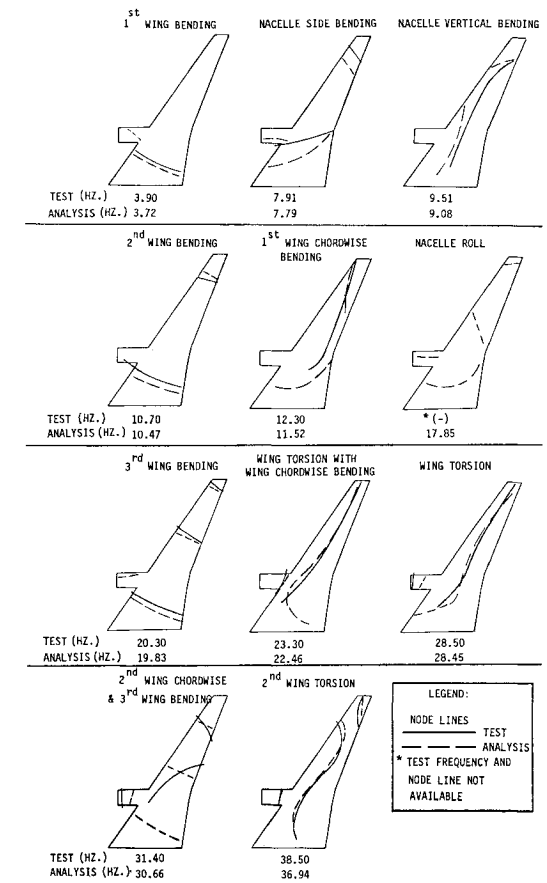

Fig. 2b Still air vibration correlation for low-speed model wing (75% fuel)/nacelle (nominal)/winglet (20 deg).

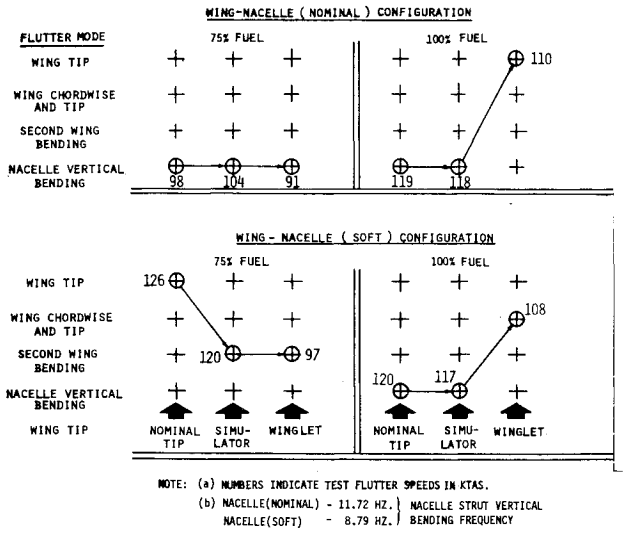

Fig. 3 Summary of low-speed flutter test results.

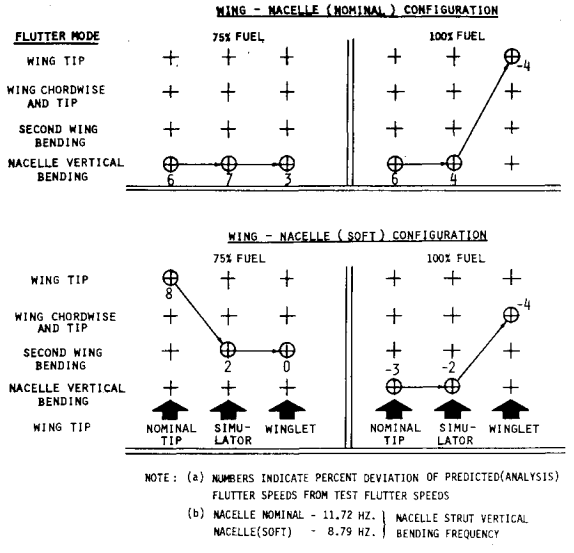

Fig. 4 Summary of low-speed test/analysis correlation.

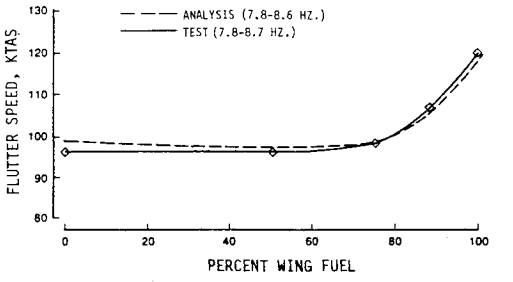

Fig. 5 Low-speed flutter test for wing/nacelle (nominal)/nominal tip.

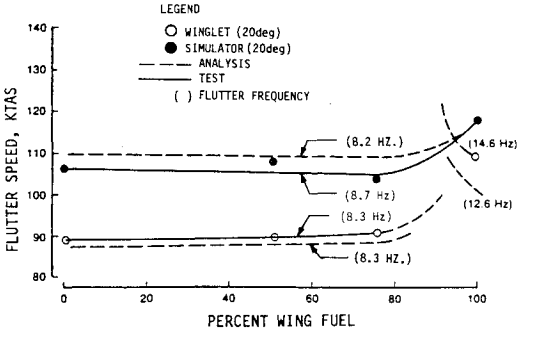

Fig. 6 Low-speed flutter test for wing/nacelle (nominal)/winglet and simulator.

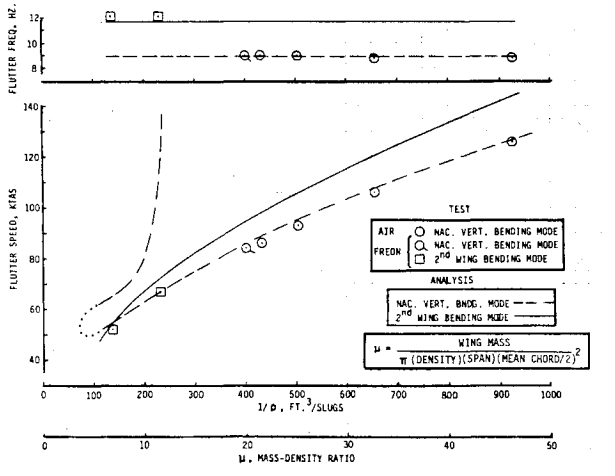

Fig. 7 Mass-density ratio effects on flutter (low-speed model) for wing (empty)/nacelle (nominal)/winglet (20 deg).

winglet aerodynamics. It appears that flutter speeds would be minimum for a cant angle which would make the winglet act as if it were a wing-tip extension. The flutter speeds did not exhibit sensitivity to winglet/simulator frequency. Angle-of-attack variation from -2 to 2 deg, and yaw angle variation from -5 to 5 deg, did not show any significant effect on flutter speed. Thus, the significant parameters for the low-speed test were 1) wing fuel, 2) nacelle vertical-bending frequency, 3) wing-tip configuration, and 4) winglet cant angle. These parameters were selected for further investigation with the high-speed model.

Flutter Correlation

The model was analyzed using conventional flutter analysis techniques. The model spar was represented by finite beam elements (elastic axis). The nacelle and strut were attached as rigid lump-masses to the wing elastic axis. The winglet and ballasted tip were modeled as separate substructures using branch mode representation. The cantilevered nacelle strut and winglet frequencies and mode shapes were input as assumed modes. The calibrated model stiffness properties were incorporated to improve correlation with the results of the model GVT. The aerodynamic representation for flutter analysis was based on strip theory aerodynamics.[10] The sectional, static aerodynamic data were derived from wind tunnel pressure tests.

Analysis of the flutter model predicted the four flutter modes described previously for appropriate configurations. Figure 4 shows the flutter modes predicted by the analysis and the percent deviation from test flutter speeds shown in Fig. 3. The flutter speed trends generally agreed with trends from the test. Figures 5 and 6 show a direct comparison of flutter speeds for the wing/nacelle, wing/nacelle/simulator, and wing/nacelle/winglet configurations. Flutter speeds for the NVB mode are plotted for structural damping (g) of 0.015; and flutter speeds for the remaining modes are for $g=0.005$. These damping values are in accordance with the model GVT results. It can be seen that the analysis/test correlation is reasonably good.

Mass-Density Ratio Effects

The low-speed model was tested in the NASA Langley TDT in both air and freon to determine mass-density ratio

effects. The two configurations tested were: the wing with nominal nacelle, and the wing with nominal nacelle and winglet (20 deg). Results for the wing with nominal nacelle and winglet (20 deg) are shown in Fig. 7. The flutter mode changed from second wing bending to nacelle vertical bending near a mass-density ratio of 15. The analysis/test correlation was reasonably good. The switch in the flutter mode occurred at a higher mass-density ratio in the test than shown by analysis. A small difference in actual and predicted damping could explain this difference.

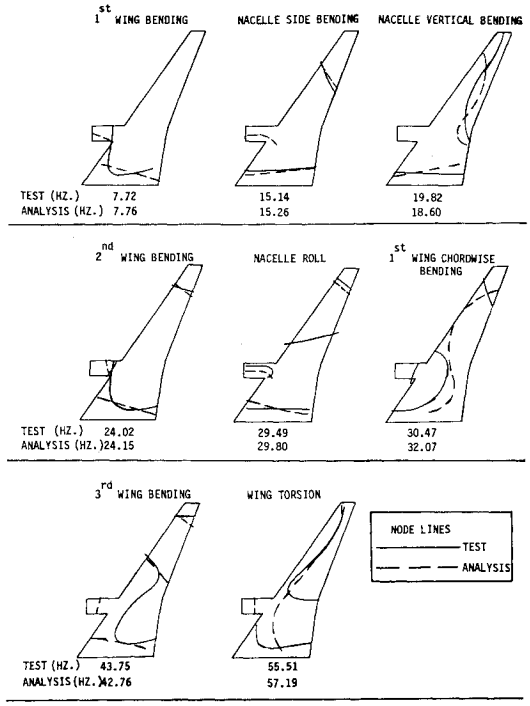

Fig. 8a Still air vibration correlation for high-speed model wing (empty)/nacelle (nominal)/nominal tip.

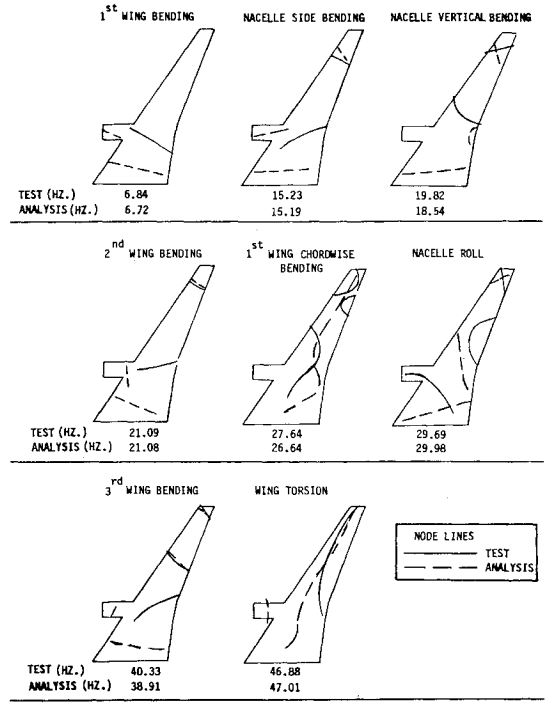

Fig. 8b Still air vibration correlation for high-speed model wing (empty)/nacelle (nominal)/winglet (20 deg).

High-Speed Flutter Results

Model GVT

The model was installed in the NASA Langley TDT, and was supported by the NASA balance mounted on the wall turntable. An extensive model ground vibration test (GVT) was performed prior to model installation in the tunnel. Figures 8a-c show the vibration analysis/test correlation for wing (empty)/nacelle (nominal)/nominal tip, wing (empty)/nacelle (nominal)/winglet (20 deg), and wing (full)/nacelle (nominal)/winglet (20 deg) configurations, respectively. Structural damping of the model varied from 0.014 to 0.025.

Flutter Test Results

The test results obtained in the NASA Langley TDT are shown in Figs. 9a-d. All configurations tested indicated a sizeable drop in flutter dynamic pressure (Q_F) due to the combined effects of Mach number and mass-density ratio, as expected. There was a significant reduction in Q_F due to the winglet aerodynamic effects. For the configuration with nominal nacelle strut and empty fuel (Fig. 9a), the effect of the ballasted tip was to slightly lower the flutter boundary except at higher Mach numbers. However, for the configuration with the nominal nacelle strut and full fuel (Fig. 9b), the ballasted tip caused a low-damped mode at a slightly lower dynamic pressure. The reduction in Q_F due to winglet aerodynamic effects was more pronounced for this case. The configuration with the soft nacelle strut and empty fuel (Fig. 9c) showed trends similar to the configuration with nominal nacelle strut. The effect of winglet cant angle shown in Fig. 9d was found to be similar to that for the low-speed model. The differences in the effects of winglet aerodynamics on different configurations were primarily due to the flutter modes. The four flutter modes encountered were similar to the four flutter mechanisms found for the low-speed model. An angle-of-attack variation series was run within model load limits for the wing (empty)/nacelle (nominal)/winglet (20 deg) configuration. No single degree-of-freedom instability was found to exist.

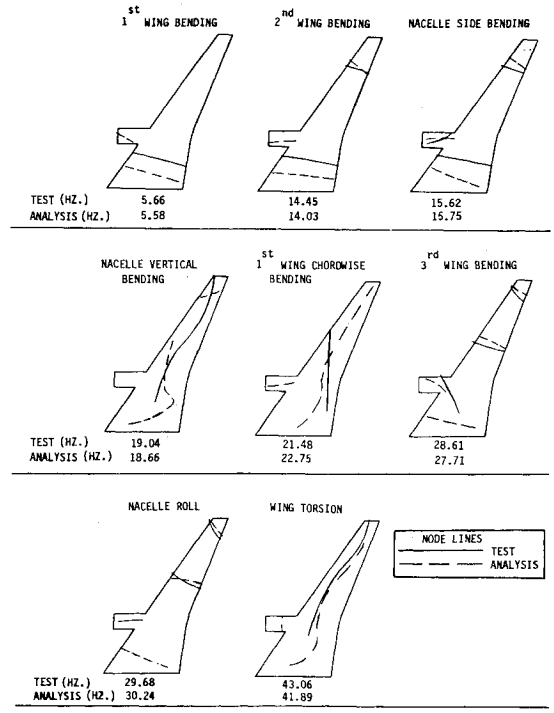

Fig. 8c Still air vibration correlation for high-speed model for wing (full)/nacelle (nominal)/winglet (20 deg).

Flutter Correlation

The analytical representation used was identical to the low-speed model. The built-up, high-speed model wing was structurally represented by finite beam elements (elastic axis) as if the wing were of single-spar construction. Strip theory aerodynamics was used with spanwise lift and moment data for each Mach number derived from the static wind tunnel test data. The analysis/test correlation obtained is shown in Figs. 10a-d for selected configurations. The analysis was found to be slightly conservative for the wing (empty)/nacelle (nominal) configuration with nominal tip (Fig. 10a), while slightly unconservative for the configuration with the ballasted tip (Fig. 10b). The correlation for the wing (empty)/nacelle (nominal)/winglet (20 deg) configuration was also considered to be satisfactory (Fig. 10c). At Mach 0.66, the model response showed high amplitude in the 17.6-Hz nacelle vertical-bending mode and the 22.3-Hz second wing-bending mode. The ratio of acceleration amplitude squared for the 22.3- to 17.6-Hz mode was 1.37. This ratio was based on a spectrum derived from exponential averaging, with overlap processing, of 10 ensembles of 5 s each. The corresponding ratio of displacement amplitudes was 0.72. Therefore, it is possible to classify the flutter mode as a second wing-bending mode based on acceleration response, or as a nacelle vertical-bending mode based on displacement response.

The wing (full)/nacelle (nominal)/winglet (20 deg) configuration results are shown in Fig. 10d. This was the most complicated configuration in terms of sorting out the flutter modes. Three flutter modes (nacelle vertical bending, wing chordwise bending, and wing tip) were observed. At Mach 0.856, there was distinct beating between the 18.5-Hz (nacelle vertical bending) and 19.1-Hz (wing chordwise bending) modes. At Mach 0.79, response in both of these modes was apparent. The higher frequency wing-tip mode was observed for the test points at Mach numbers of 0.73 and 0.644. The analytical results matched well for the nacelle vertical-bending and wing chordwise mode at the two higher Mach numbers. However, the analysis appears conservative for the wing chordwise mode and unconservative for the wing-tip mode.

An analytical sensitivity study was conducted to evaluate the effect of selected parameters on analysis/test correlation. The primary configuration for the sensitivity study was the wing (full)/nacelle (nominal)/winglet (20 deg) configuration. This was judged to be the most interesting configuration tested since three flutter mechanisms were observed. It was found to be sensitive to the characteristics of the wing chordwise bending. This sensitivity was due to the significant wing-tip bending and torsion motion in the wing chordwise mode. The sensitivity to aerodynamic sectional data was as normally would be expected.

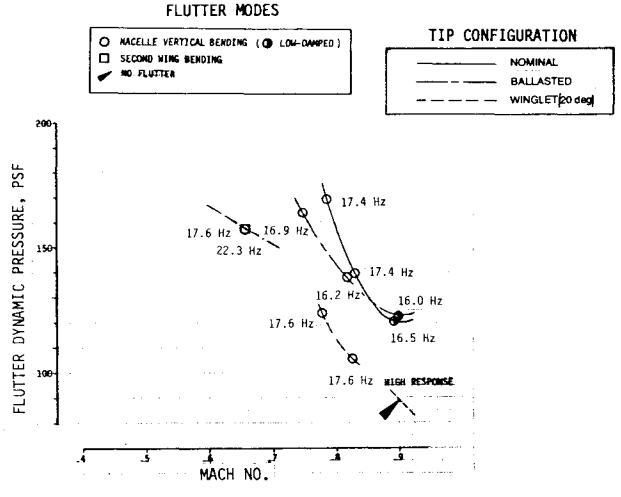

Fig. 9a Effect of wing-tip configuration on test flutter boundary for wing (empty)/nacelle (nominal).

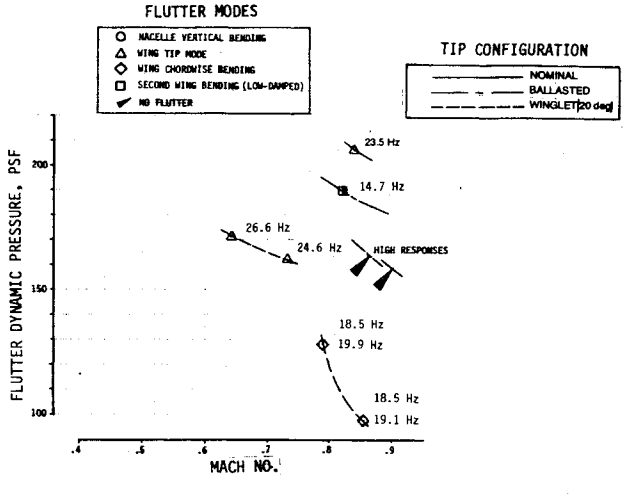

Fig. 9b Effect of wing-tip configuration on test flutter boundary for wing (full)/nacelle (nominal).

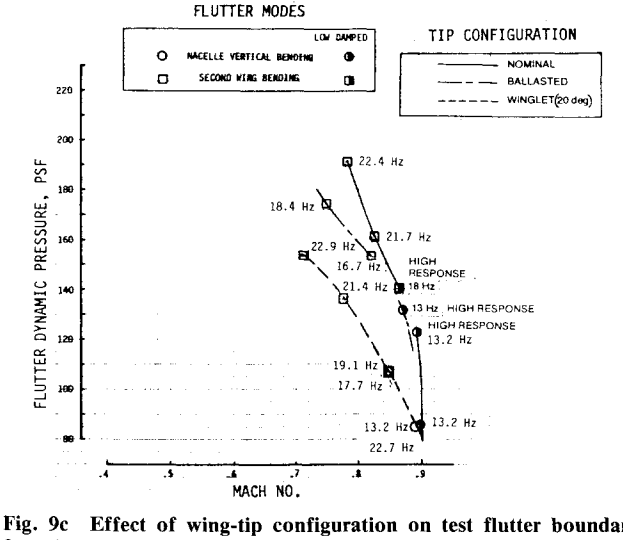

Fig. 9c Effect of wing-tip configuration on test flutter boundary for wing (empty)/nacelle (soft).

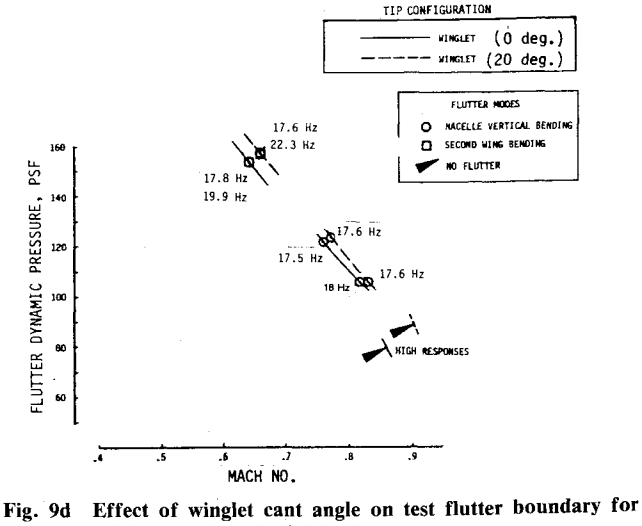

Fig. 9d Effect of winglet cant angle on test flutter boundary for wing (empty)/nacelle (nominal)/winglet.

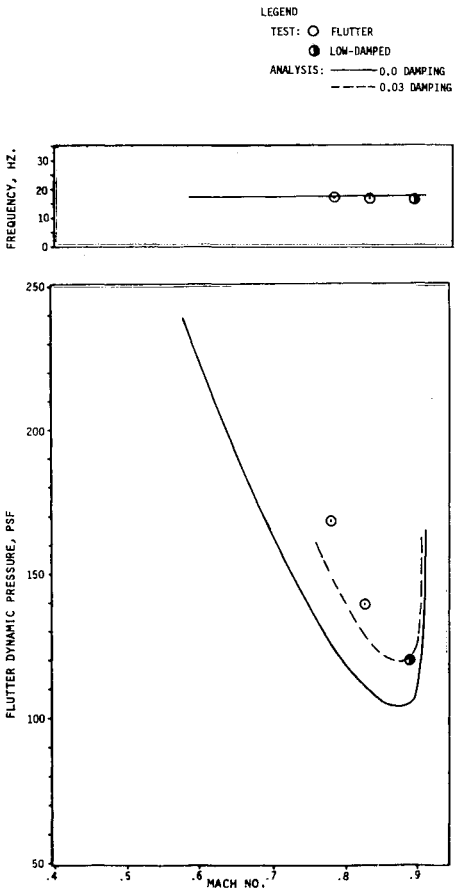

Fig. 10a Flutter correlation for wing (empty)/nacelle (nominal)/ nominal tip.

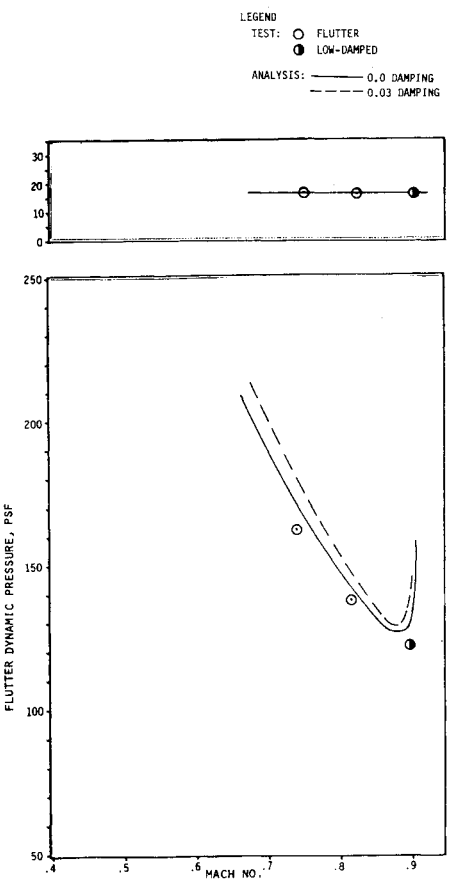

Fig. 10b Flutter correlation for wing (empty)/nacelle (nominal)/ ballasted tip.

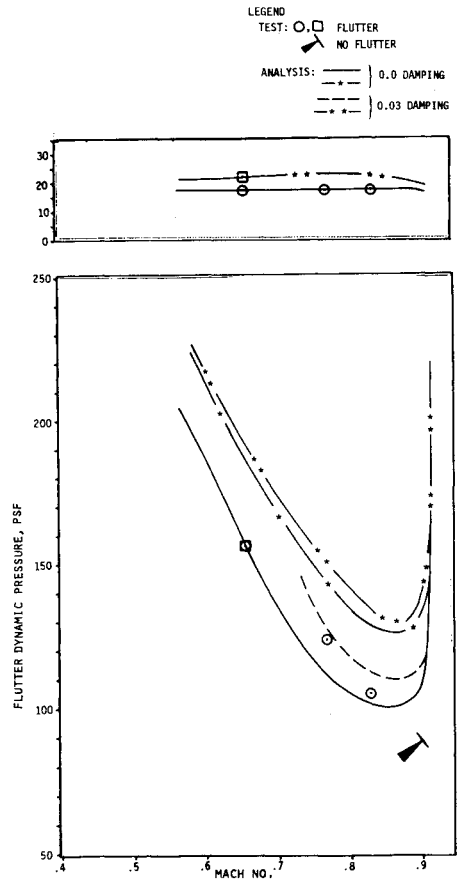

Fig. 10c Flutter correlation for wing (empty)/nacelle (nominal)/ winglet (20 deg).

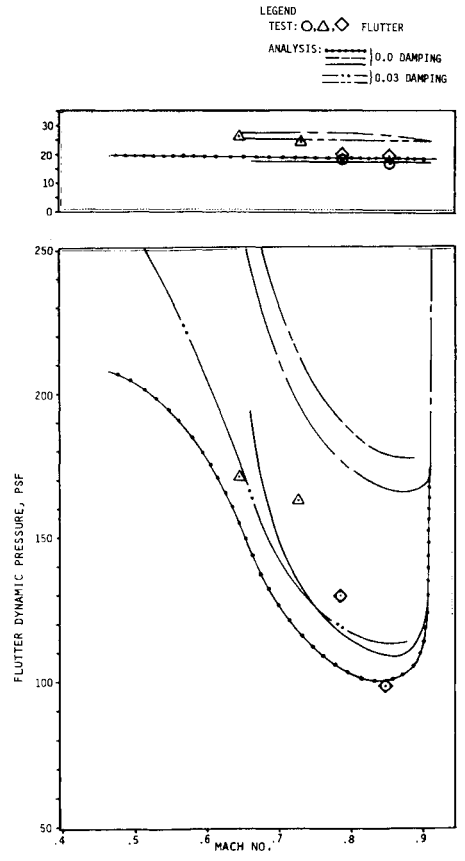

Fig. 10d Flutter correlation for wing (full)/nacelle (nominal)/ winglet (20 deg).

Conclusions

The experimental database created in this program can be used for evaluation of different theoretical approaches. The presence of the winglet caused reduction in flutter speed in both the flutter model test and analysis. The four flutter mechanisms predicted by analysis were observed in the test. The number of flutter test points obtained in the tunnel cover a wide range of configurations, altitudes, and Mach numbers. This provides an excellent reference for evaluation of analytical correlation for a configuration with or without winglets.

The mass-density ratio effects at low Mach numbers were correlated (analysis vs test) satisfactorily over a wide range. The application of conventional analysis techniques proved to be satisfactory through the transonic Mach regime. No single-degree-of-freedom flutter mechanism was found to exist. It was concluded that the flutter characteristics of a winglet configured high aspect ratio wing can be predicted satisfactorily with careful application of existing methods for a wind tunnel model of a twin-engine airplane configuration.

Acknowledgment

The authors wish to acknowledge the contributions of the following Boeing personnel to this study: J. F. Bueno, A. W. Byrski, W. F. Carver, M. G. Friend, J. L. Hill, R. G. Kunkell, D. W. Lee Jr., D. J. Marzano, J. E. Morrison, R. M. Nadreau, C. R. Pickrel, S. Ros, J. L. Stelma, and J. H. Thompson.

References

[1]Whitcomb, R. T., "A Design Approach and Selected Wind-Tunnel Results at High Subsonic Speeds for Wing-Tip Mounted Winglets," NASA TN D-8260, July 1976.

[2]Ishimitsu, K. K., "Aerodynamic Design and Analysis of Winglets," AIAA Paper 76-940, Sept. 1976.

[3]Kehoe, M. W., "KC-135 Winglet Program Review," NASA CP 2211, Sept. 1981.

[4]"Selected Advanced Aerodynamics and Active Controls Technology Concept Development on a Derivative B-747 Aircraft," NASA CR 3164, Feb. 1980.

[5]Ruhlin, C. L., Rauch, F. J., and Waters, C., "Transonic Flutter Model Study of a Supercritical Wing and Winglet," *Journal of Aircraft*, Vol. 20, Aug. 1983, pp. 711-716.

[6]Schollenberger, C. A., Humpherys, J. W., Heiberger, F. S., and Pearson, R. M., "Results of Winglet Development Studies for DC-10 Derivatives," NASA CR 3677, 1983.

[7]"DC-10 Winglet Flight Evaluation," NASA CR 3704, May 1983.

[8]Bhatia, K. G. and Nagaraja, K. S., "Flutter Parametric Studies of Cantilevered Twin-Engine-Transport Type Wing Models with and without Winglets," Vols. I and II, NASA CR 172410, Sept. 1984.

[9]Ruhlin, C. L., NASA TP to be published, 1985.

[10]Dreisbach, R. L., ed., "ATLAS—An Integrateral Structural Analysis and Design System, ATLAS User's Guide," NASA CR-159041, July 1979.